Short Note

(3-(4-chlorophenyl)-4,5-dihydroisoxazol-5-yl)methyl Benzene-Sulfonate

Loubna Mokhi , Karim Chkirate , Xiaodong Zhang , Mohsine Driowya , Khalid Bougrin *

Posted Date: 11 September 2023

doi: 10.20944/preprints202309.0671.v1

Keywords: Green strategy; One-pot reaction; isoxazoline sulfonate; Ultrasound cavitation; X-ray single-crystal structure analysis; Hydrogen bond; Hirshfeld surface analysis; DFT calculation.

Short Note

(3-(4-chlorophenyl)-4,5-dihydroisoxazol-5-yl)methyl Benzene-Sulfonate

Loubna Mokhi [1], Karim Chkirate [2], Xiaodong Zhang [3], Mohsine Driowya [1,4] and Khalid Bougrin [1,5,*]

1 Equipe de Chimie des Plantes et de Synthèse Organique et Bioorganique, URAC23, Faculty of Science, B.P. 1014, Geophysics, Natural Patrimony and Green Chemistry (GEOPAC) Research Center, Mohammed V University in Rabat, Rabat 10010, Morocco; loubna.mokhi@um5r.ac.ma (L.M.); k.bougrin@um5r.ac.ma (K.B.)
2 Laboratory of Heterocyclic Organic Chemistry URAC 21, Pharmacochemistry Competence Center, Av. Ibn Battouta, BP 1014, Faculty of Sciences, Mohammed V University in Rabat, Rabat 10010, Morocco; k.chkirate@um5r.ac.ma (K.C.)
3 Department of Chemistry, Tulane University, New Orleans, LA 70118, USA; xzhang2@tulane.edu (X.Z.)
4 Higher School of Technology, Sultan Moulay Slimane University, B.P. 170, Khenifra 54006, Morocco; m.driowya@usms.ma (M.D.)
5 Chemical & Biochemical Sciences Green-Process Engineering (CBS), Mohammed VI Polytechnic University, Lot 660, Hay Moulay Rachid, Ben Guerir 43150, Morocco
* Correspondence: k.bougrin@um5r.ac.ma

Abstract: A novel single crystal (3-(4-chlorophenyl)-4,5-dihydroisoxazol-5-yl)methyl benzenesulfonate has been synthetized via a one-pot sequential strategy under sonication. The single crystal has been investigated using X-ray diffraction analysis. Hydrogen bonding between C—H···O and C—H···N produce a layer structure in the crystal. According to a Hirshfeld surface analysis, interactions H···H (28.9%), H···O/O···H (26.7%) and H···C/C···H (15.8%) make the biggest contributions to crystal packing. The optimized structure and the solid-state structure that was obtained through experimentare compared using density functional theory at the B3LYP/6-311 G+(d,p) level. The computed en-ergy difference between the lowest unoccupied molecular orbital (LUMO) and highest occupied molecular orbital (HOMO) is 4.6548 eV.

Keywords: green strategy; one-pot reaction; isoxazoline sulfonate; ultrasound cavitation; X-ray analysis; hydrogen bond; hirshfeld surface; DFT

1. Introduction

Compounds bearing isoxazoline moiety are considered an significant class of nitrogen and oxygen atoms containing heterocyclic products, attracting attention from organicand medicinal chemists due to their large spectrum of biological properties such as antibacterial [1,2], antimicrobial [3], anti-inflammatory [4], anticancer [5,6], antidiabetic [7] and anti-Alzheimer [8]. Moreover, isoxazoline derivatives are also known by their agrochemical properties as herbicidal [9], insecticidal [10–12] and acaricidal agents [13]. On the other hand, sulfonic esters are clearly identified for their crucial role in the synthesis of organic compounds and have shown interesting pharmacological properties in the past decade [14–16]. Accordingly, the synthesis of molecules containing both isoxazoline and sulfonate ester scaffolds providing easy access to a range of well-defined bioactive compounds for complete chemical, biochemical and pharmacological research [17,18]. On this account, several methods are reported for the preparation of isoxazoline systems [19,20].

However, 1,3-dipolar cycloaddition which involves alkene as dipolarophile and nitrile oxide as dipole remains as one the most attractive route to prepare this aza-heterocycle [21]. As for the sulfonate ester synthesis, the most common protocol for its preparation is the reaction of sulfonyl chlorides with alcohols by using of a base [22]. In this study, we 4described the preparation and structural determination of new isoxazoline-linked sul fonate compound utilizing an efficient and

Preprints (www.preprints.org) | NOT PEER-REVIEWED | Posted: 11 September 2023 doi:10.20944/preprints202309.0671.v1

green protocol in water under ultrasound cav itation, which emerges as a suitable alternative to previously reported methods for the organic synthetic laboratory [23,24]

In addition to evaluating a molecule's activity, theoretical calculations provide valuable knowledge on a variety of a molecule's characteristics [25]. With the development of technology, calculated results have gotten more precise and faster [25]. Considering the variety of uses mentioned above, the title compound [3-(4-chlorophenyl)-4,5-dihydroisox-azol-5-yl]methyl benzenesulfonate was prepared and identified spectroscopically. The three-dimensional structure was resolute by single-crystal X-ray diffraction investigation. To determine the compound's optimal molecular structure characteristics, HOMO-LUMO energies, and thermodynamic parameters, Hirshfeld surface analysis and density functional theory (DFT) computations were used to study the intermolecular interactions and hydrogen bonds. In this study, the chemical properties of the molecules were investigated employing 6-311+ g(d,p) basis set and B3LYP techniques with Gaussian calculations.

2. Results

2.1. Synthesis

Inspired from our previous works [26,27], the one-pot synthesis of our product (**5**) started by the sulfonylation of equimolar equivalent of allylic alcohol (**1**) and benzene sulfonyl chloride (**2**) in water with NaOH as a base at 25 °C under sonication to give in situthe corresponding dipolarophile (**3**). Subsequently, in the second step, the alkene sulfonate (**3**) reacts with p-chlorobenzaldoxime (**4**) via 1,3-dipolar cycloaddition using NaCl as a precatalyst generated from the first step and oxone as a terminal oxidant to afford successfully the expected (3-(4-chlorophenyl)-4,5-dihydroisoxazol-5-yl)methyl benzenesulfonate (**5**) as white crystals in 85% yield (Scheme 1).

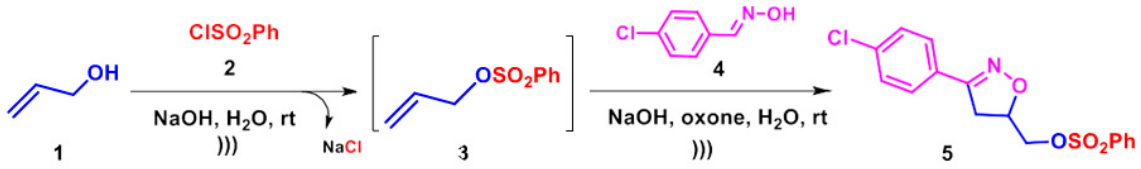

Scheme 1. One-pot synthesis of compound **5**.

The structure of isoxazoline sulfonate (**5**) was fully characterized by FT-IR, ^{1}H NMR, ^{13}C NMR and ESI^{+}-MS spectroscopies, and confirmed by single-crystal X-ray diffraction (See Supplementary Materials (*SM*) section). As illustrated in Figure 1, the ^{1}H NMR spectrum of (**5**) showed two doublets of doublet at 3.47 and 3.12 ppm corresponding to the two protons of the CH_2-isoxazolinic as well as two doublets of doublets at 4.14 and 4.19 ppm for the O-CH_2 protons. Furthermore, we detected the presence of a multiplet centered at 4.92 ppm illustrating the H-isoxazolinic proton. Then, the region between 7.47 and 7.88 ppm showed the signals of the different aromatic protons. The ^{13}C NMR spectrum exhibit three blinded signals at 36.6, 71.6 and 78.5 ppm corresponding subsequently to CH_2-isoxazoline, O-CH_2 and CH-isoxazoline and signals at 156.3, 135.5, 135.3, 135.0, 130.3(2C), 129.4(2C), 128.9(2C), 128.3, 128.2(2C) attributed to all the aromatic carbons.

Preprints (www.preprints.org) | NOT PEER-REVIEWED | Posted: 11 September 2023 doi:10.20944/preprints202309.0671.v1

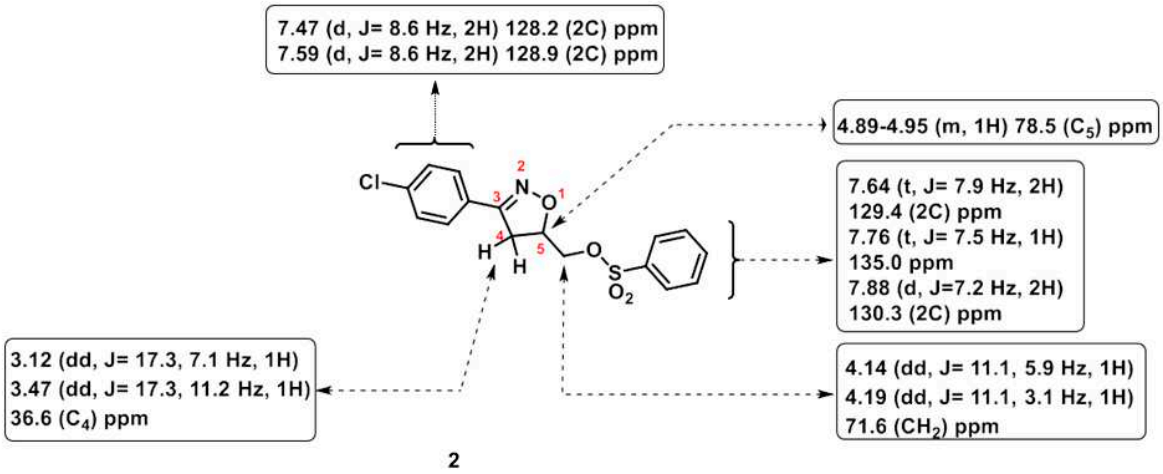

Figure 1. Characteristic ^{1}H, ^{13}C NMR of compound (**5**).

2.2. X-ray Analysis

X-ray intensity data were collected at 150(2) K. Using APEX4 [28], the structure was solved via Intrinsic Phasing in the SHELXT [29] structure solution program and refined using Least Squares minimization in the SHELXL [30] refinement package. With one molecule in the asymmetric unit, the [3-(4-chlorophenyl)-4,5-dihydroisoxazol-5-yl]methylbenzenesulfonate crystallizes in the orthorhombic space group Pbca (Figure 2).

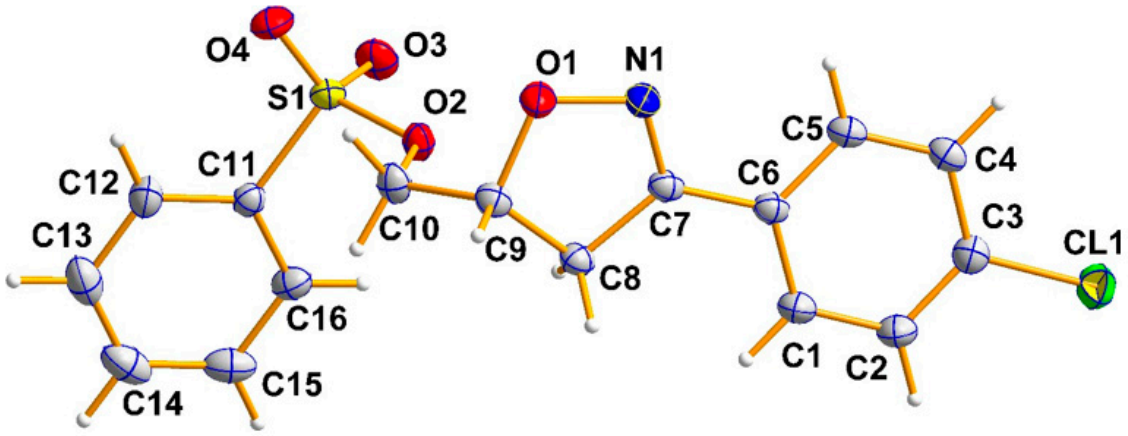

Figure 2. The title molecule with labeling scheme and 50% probability ellipsoids.

The molecules are linked by a small C—H···O contact (Figure 3) and by short C—H···N contacts to form a long chain along the a-axis (Figure 4). Molecules are linked in crystallographic symmetry in a unit cell by eight molecules forming four pairs by connection by short C—H···O contacts (represented by blue dotted lines). Each pair will form a long chain along the a-axis through the C—H···N interactions (not shown). The four long chains interact with each other through C—H···π(ring) and C—O···π(ring) interactions, which are represented by black dotted lines (with centroids shown as of pink spheres) (Figure 5 and Table 1).

Preprints (www.preprints.org) | NOT PEER-REVIEWED | Posted: 11 September 2023 doi:10.20944/preprints202309.0671.v1

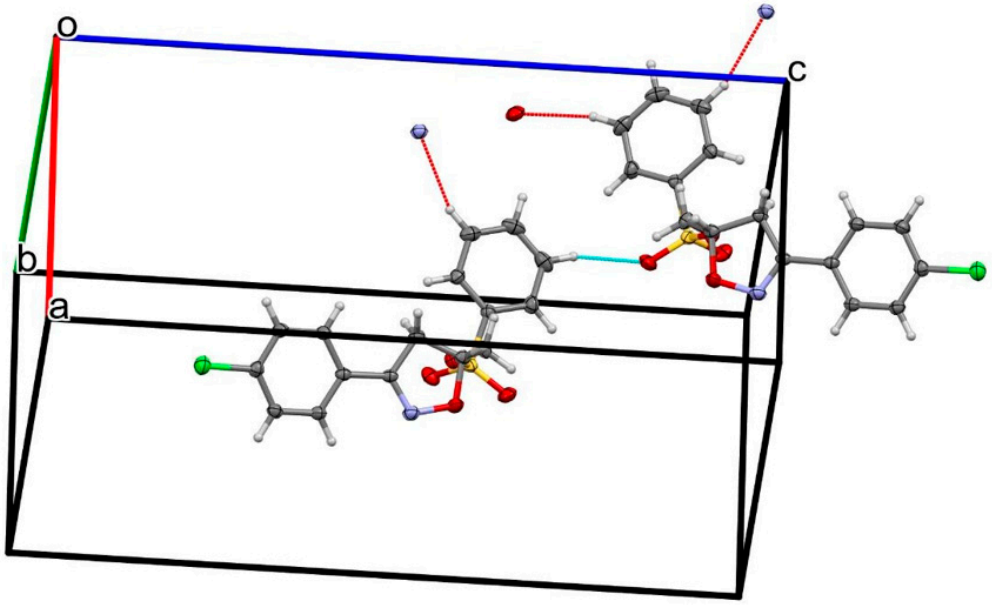

Figure 3. This picture shows two molecules connected through C—H···O short contact to form a pair.

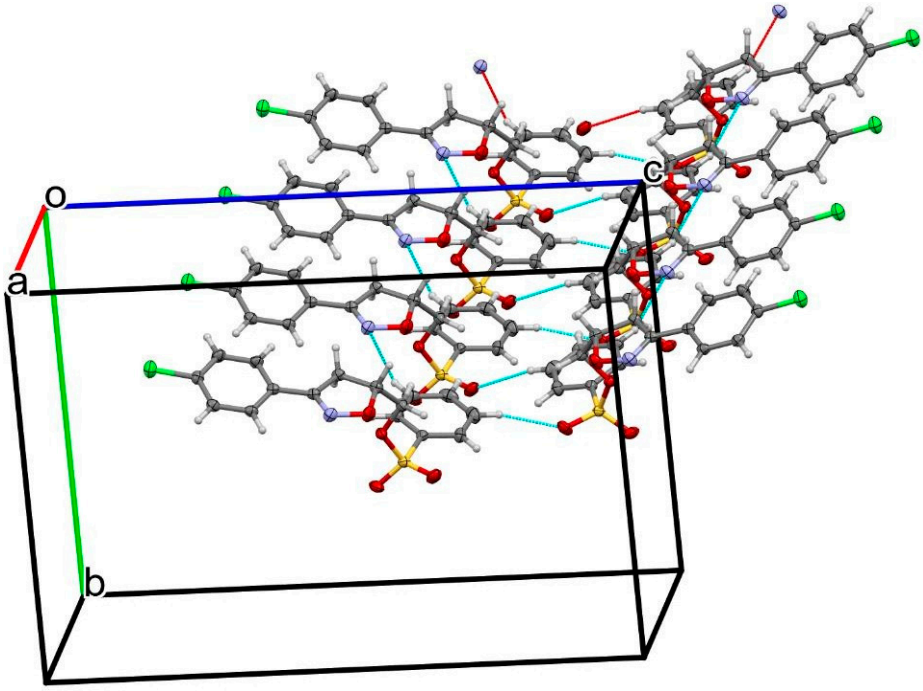

Figure 4. This picture shows many pairs of molecules are connected through C—H···N short contacts to form a long chain along a-axis.

Preprints (www.preprints.org) | NOT PEER-REVIEWED | Posted: 11 September 2023 doi:10.20944/preprints202309.0671.v1

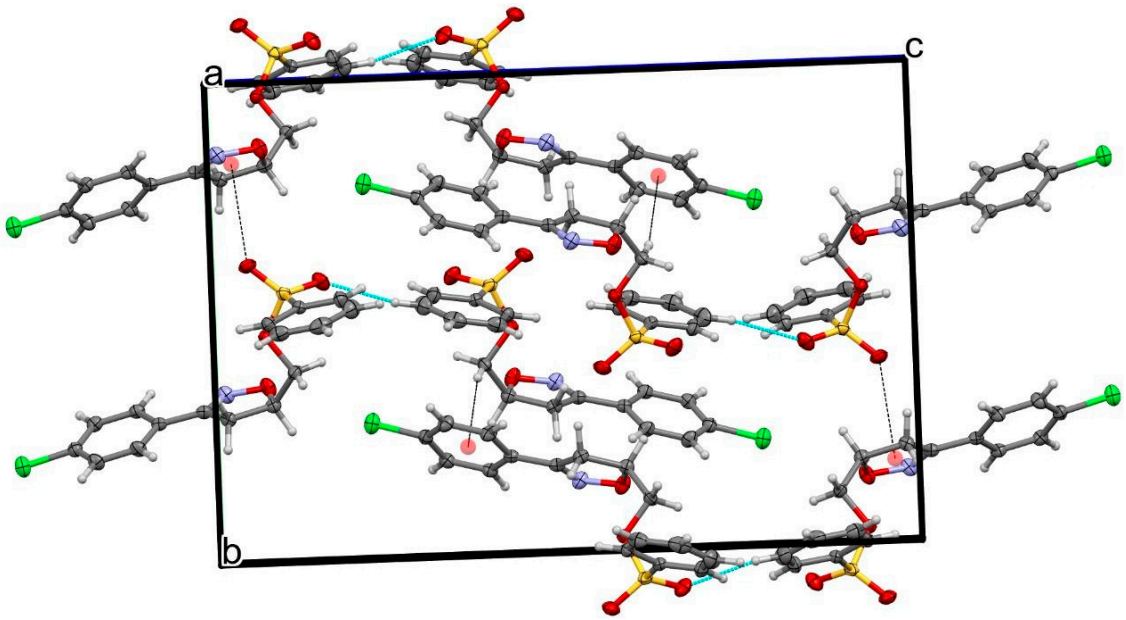

Figure 5. This picture shows eight crystallographic symmetry related molecules in one-unit cell.

These molecules form four pairs through connection by C—H···O short contacts (depicted as blue dashed lines). Each pair will form a long chain along a-axis through C—H···N interactions (not shown). The four long chains interact with each other through C—H···π(ring) and C—O···π(ring) interactions, which are depicted as black dashed lines (with centroids displayed as pink spheres).

Table 1. Hydrogen bond geometries (Å, °) for [3-(4-chlorophenyl)-4,5-dihydroisoxazol-5-yl]methyl benzenesulfonate.

D—H···*A*	*D*—H	H···*A*	D···*A*	*D*—H···*A*
C2—H2···Cl1^{i}	0.95	2.84	3.5624 (11)	133.2
C4—H4···O4^{ii}	0.95	2.59	3.2807 (12)	129.5
C16—H16···O2^{iii}	0.95	2.61	3.4229 (12)	144.1
C16—H16···O3^{iii}	0.95	2.61	3.4416 (13)	146.5

Symmetry codes: (i) *x*−1/2, *y*, −*z*+1/2; (ii) −*x*+2, −*y*+1, −*z*+1; (iii) −*x*+1, −*y*+1, −*z*+1.

Crystal Explorer 17.5 [31–33] was used to conduct a Hirshfeld surface (HS) analysis in order to see how [3-(4-chlorophenyl)-4,5-dihydroisoxazol-5-yl]methyl benzenesulfonate interacts with other molecules in the crystal. As shown in Figure 6a, the blue and red colors surface in the HS plotted over d_{norm} denote contacts with distances that are longer (distinct contact) or shorter (in close contact), respectively, whereas the white de- 123 notes connections with distances equal to the sum of van der Waals radii. The most im- 124 portant red spots and the corresponding interactions are shown in Figure 7. The shape- 125 index (Figure 6b) generated in the range -1 to 1 Å shows that there are no π– π interactions, normally indicated by adjacent blue and red triangles. The sites of intimate intermolecular contacts in the compound are clearly visible in the potential electrostatic calculated utilizing the STO-3G basis, mapped on the Hirshfeld surface throughout the range of 0.05 a.u., set at the Hartree-Fock level of theory (Figure 6c). Positive potential electrostatic (blue zone) over the surface denotes hydrogen-donor potential, whereas negative electrostatic potential (red region) denotes hydrogen-bond acceptors.

Preprints (www.preprints.org) | NOT PEER-REVIEWED | Posted: 11 September 2023 doi:10.20944/preprints202309.0671.v1

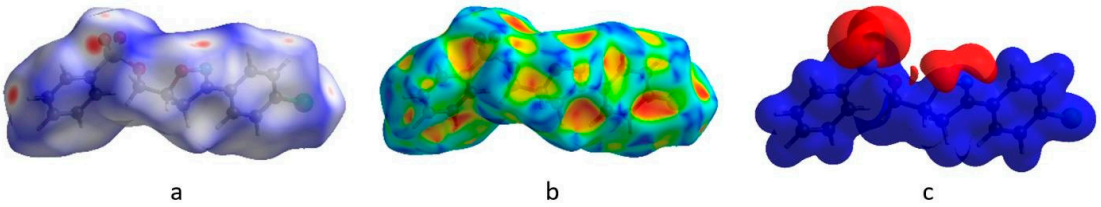

Figure 6. View of the Hirshfeld surface of [3-(4-chlorophenyl)-4,5-dihydroisoxazol-5-yl]methyl benzenesulfonate. (a) mapped over dnorm in the range -0.2185 to 1.3206 a.u., (b) over shape-index mapped. (c) Electrostatic potential energy in the range -0.05 to 0.05 a.u. mesured using the STO-3 G basis set at the Theoretical level of Hartree-Fock.

Figure 7 depicts the existence of multiple brilliant red spots on the three-dimensional d_{norm} surfaces of the crystal structure, which are hydrogen bonding interactions.

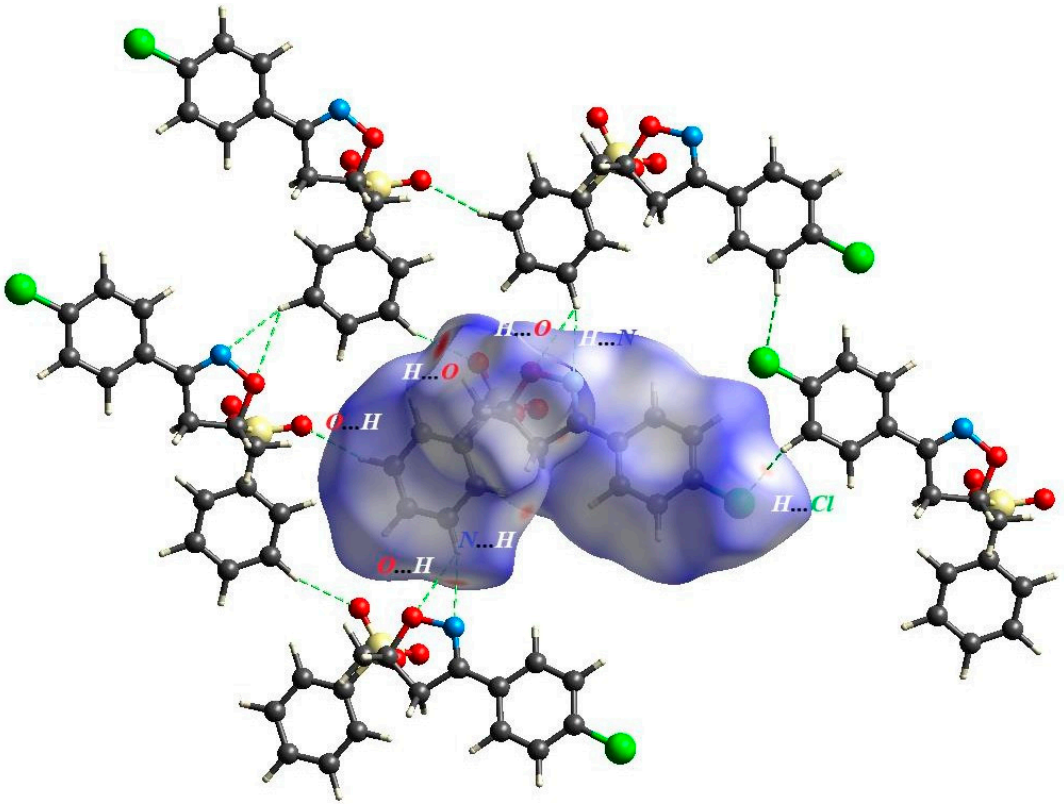

Figure 7. Principal non-covalent interactions and the Hirshfeld surface are plotted over dnorm in the crystal packing of [3-(4-chlorophenyl)-4,5-dihydroisoxazol-5-yl]methyl benzenesulfonate.

Figure 8a displays the entire two-dimensional fingerprint pattern [34], while those divided into H···O/O···H, H···H, H···C/C···H, H···Cl/Cl···H, H···N/N···H, C···C, Cl···O/O···Cl and O···C/C···O contacts are illustrated in Figure 8b–i, respectively, and their relative contributions to the Hirshfeld surface (HS). Given the high hydrogen content of the molecule and its significant contribution of 28.9% to the total crystal packing, the most significant interaction is HH, which is depicted in Figure 8b as widely scattered points of high density with a tip at $d_e = d_i = 1.28$ Å. The tips of the pair of distinctive wings in the fingerprint plot demarcated into H···O/O···H interactions (26.7%), Figure 8c, are at $d_e + d_i = 2.22$ Å when O—H interactions are present. The tips of the two distributed points of spikes in Figure 8d (15.28%), the fingerprint plot demarcated into C···H/H···C, are at de + di = 2.74 Å. The Cl···H/H···Cl contacts, Figure 8e (12.8%), have the tips at $d_e + d_i = 2.73$ Å. The N···H/H···Nconnections, Figure 8f, appear as scattered dots with spikes at $d_e + d_i = 2.42$ Å and contribute 6.3% to the HS. The C···C contacts, Figure 8g, are a pair of distributed spike points with tips at $d_e + d_i = 3.31$ Å and contribute 6.2% to the HS. The Cl···O/O···Cl connections, Figure 8h, a pair of scattered spike tips emerge with a

Preprints (www.preprints.org) | NOT PEER-REVIEWED | Posted: 11 September 2023 doi:10.20944/preprints202309.0671.v1

tip at de + di = 3.42 Å and contribute 1.9% to the HS. The O···C/C···O contacts, Figure 8i, have a low point density and only contribute 0.7% of the total points to the HS.

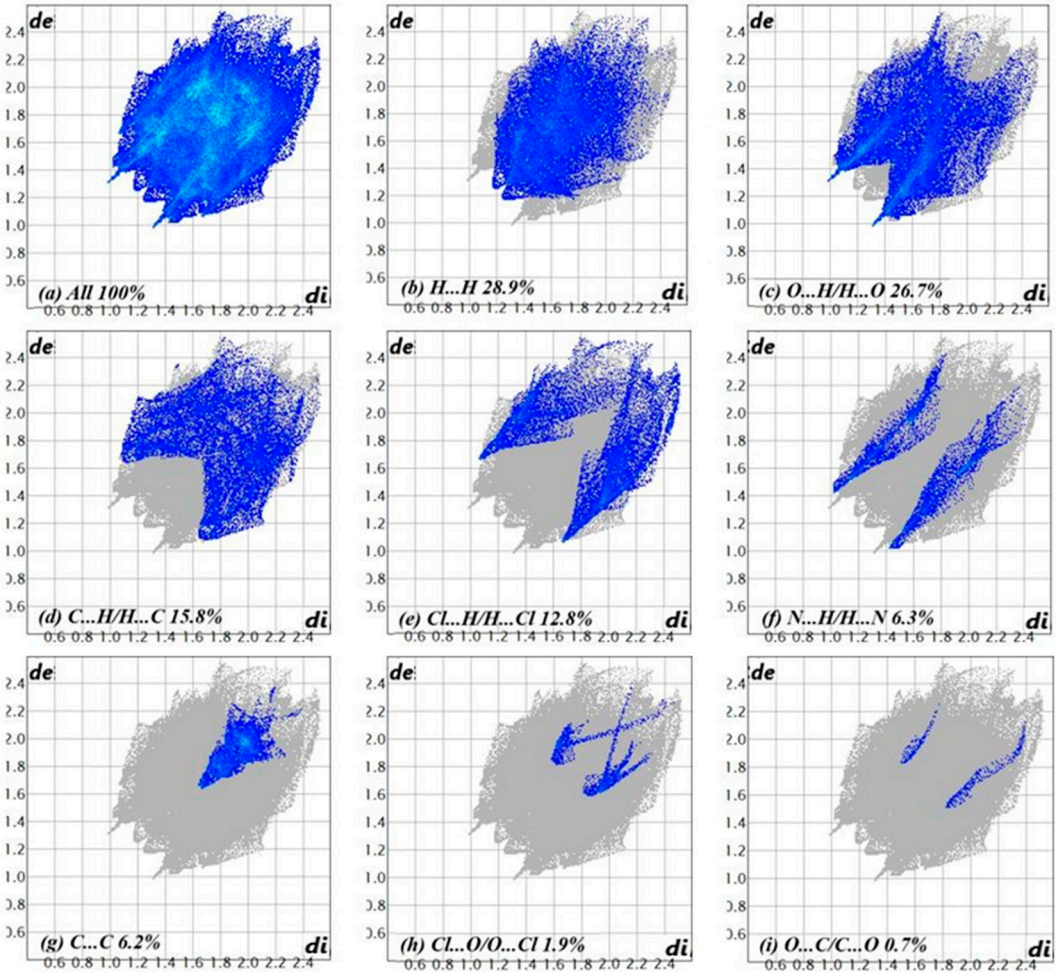

Figure 8. Two-dimensional fingerprint plots for the title compound, showing (a) all interactions, and delineated into (b). H···H, (c) H···O/O···H, (d) C···H/H···C, (e) Cl···H/H···Cl, (f) N···H/H···N, (g) C···C, (h) Cl···O/O···Cl and (i) O···C/C···O interactions. The d_e and d_i values are the closest external and internal distances (in Å) from given points on the HS.

2.3. Theoretical Calculation Details

DFT was used to optimize the structure of [3-(4-chlorophenyl)-4,5-dihydroisoxazol-5-yl]methyl benzenesulfonate in the gas phase. The 6-311 G+(d,p) basis-set and the hybrid B3LYP method, which are built on the model of Becke [35] and take into account a combination of the exact (Hartree-Fock) and using the B3 functional DFT exchange, as well as the LYP correlation functional [36], were used to calculate the DFT. The harmonic frequencies of vibration were estimated after getting the converged geometry at the same theoretical level to verify that the stationary point has no imaginary frequencies. The GAUSS- 170IAN 09 program was used to optimize the shape and analyze the harmonic vibrational frequency of [3-(4-chlorophenyl)-4,5-dihydroisoxazol-5-yl]methyl benzenesulfonate [37]. 172 Numerous quantum chemical parameters have been discovered as a result of these studies. Each parameter describes a particular molecule's chemical characteristic [38]. Table 2 provides an overview of the experimental and theoretical findings regarding angles and bond lengths. Table 3 summarizes the results for the title compound, which include hardness (η), electronegativity (χ), ionization potential (I), electron affinity (A), dipole moment(μ), softness (σ) and electrophilicity (ω). The highest occupied molecular orbital (HOMO)and lowest unoccupied molecular orbital (LUMO) properties of the molecules are more significant than the others [39]. Figure 9 depicts the electron's change in energy level from HOMO to LUMO. The figure's brown and green areas correspond to

Preprints (www.preprints.org) | NOT PEER-REVIEWED | Posted: 11 September 2023 doi:10.20944/preprints202309.0671.v1

molecular orbitals with diametrically opposed phases. The molecule's positive phase is depicted in green, and its negative phase in brown. In the plane that spans the entire [3-(4-chlorophenyl)-4,5-dihydroisoxazol-5-yl]methyl benzenesulfonate system, the LUMO and HOMO are localized. The molecule's energy band gap is 4,6548 eV [$\Delta E = E_{LUMO} - E_{HOMO}$], and the frontier 185molecular orbital energies, E_{LUMO} and E_{HOMO}, are -1,9053 and -6,5601 eV, respectively.

Table 2. Similarity (DFT and X-ray) of selected Angles and bond lengths (°, Å).

	X-ray	B3LYP/6–311G+(d,p)
S1-O4	1.4318(8)	1.4564
S1-O3	1.4304(8)	1.4566
S1-O2	1.5791(7)	1.6509
S1-C11	1.7534(9)	1.7867
C10-O2	1.4573(11)	1.4522
C9-O1	1.4609(12)	1.4564
N1-O1	1.4126(11)	1.3954
N1-C7	1.2845(12)	1.2827
C3-Cl1	1.7445(10)	1.7562
S1-C11-C12	120.00(7)	118.8948
S1-C11-C16	118.24(7)	118.9752
C11-S1-O4	109.17(5)	110.1399
C11-S1-O3	110.00(5)	109.829
O4-S1-O3	119.42(5)	120.2536
O4-S1-O2	109.46(5)	108.1129
S1-O2-C10	117.55(6)	116.2247
C10-C9-O1	108.18(8)	106.9904
C9-O1-N1	109.36(7)	109.628
O1-N1-C7	109.72(8)	110.3487
N1-C7-C8	114.14(8)	113.2056
N1-C7-C6	121.07(8)	121.4667
C4-C3-Cl1	119.91(7)	119.4282
C2-C3-Cl1	118.44(8)	119.5688

Table 3. Calculated energies.

Molecular Energy	Title Product
Total Energy TE (eV)	-49861,0176
EHOMO (eV)	-6,5601
ELUMO (eV)	-1,9053
Gap, ΔE (eV)	4,6548
Dipole moment, μ (Debye)	6.4787
Ionization potential, I (eV)	6,5601
Electron affinity, A	1,9053
Electronegativity, χ	4,2327
Hardness, η	2,3274
Electrophilicity, index ω	3,8489
Softness, σ	0,4297
Transfer of a fraction of an electron, ΔN	0,5945

Preprints (www.preprints.org) | NOT PEER-REVIEWED | Posted: 11 September 2023 doi:10.20944/preprints202309.0671.v1

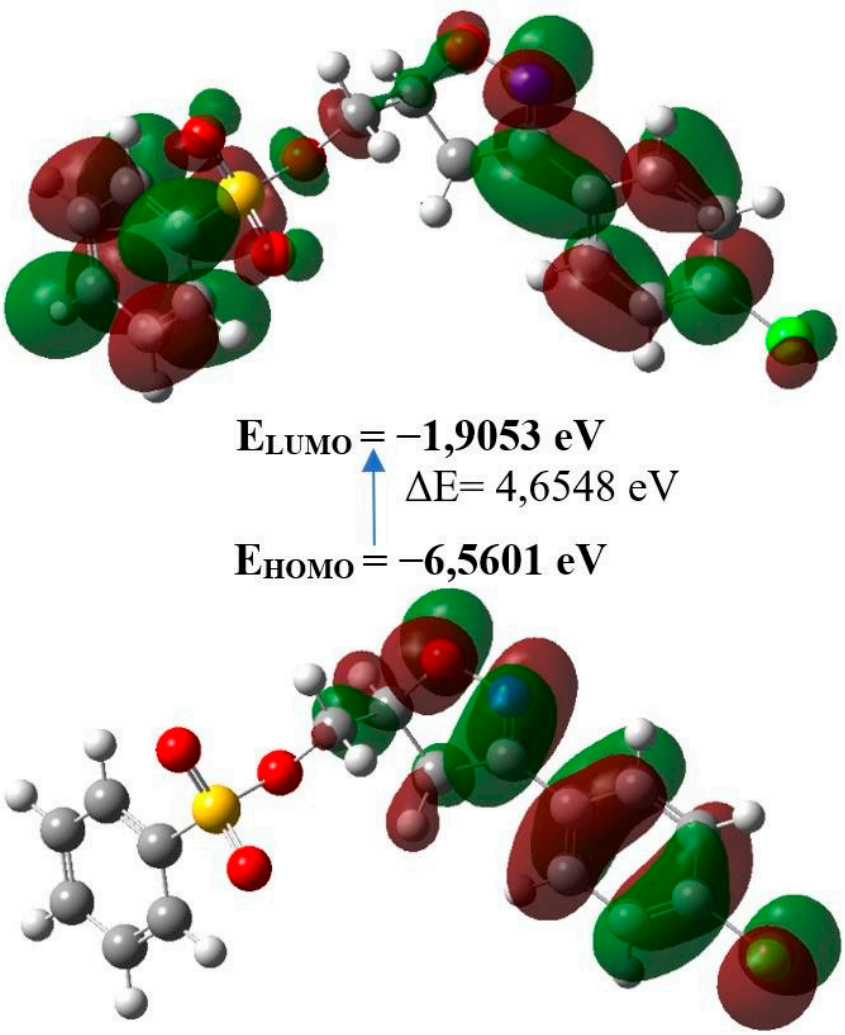

Figure 9. The energy band gap of [3-(4-chlorophenyl)-4,5-dihydroisoxazol-5-yl]methyl benzenesulfonate.

3. Experimental Section

3.1. Materials and Methods

All reactions has been followed by thin layer chromatography (precoated sheets, Silica gel 60 F254, E. Merck), and chromatograms were viewed using UV- lights at 254 and 360 nm, ^{1}H and ^{13}C NMR spectra were run in dry deuterated dimethylsulfoxyde ($DMSOd_6$) on a JNM-ECZ 500 spectrometer at 500 MHz for ^{1}H NMR and 126 MHz for ^{13}C NMR, The samples were diluted in CH_3CN, then mass spectra (ESI^+-MS) were determined on an Agilent Technologies 1260 Infinity II LC/MSD. Melting points were measured using a Köfler Bench equipment. The reactions were sonicated using a Vibra-Cell™ ultrasonic processor model 75022 with Titanium alloy Ti6Al-4 V probe (20 kHz, 130 W) and diameter of 4 mm tip; and assisted with 60% of Pmax. The sonotrode was submerged into the solution in a conical bottom flask of 25mL in order to obtain the most energy.

3.2. Preparation of Compound ***5***

In a conical bottom flask, allylic alcohol (1mmol) was introduced to a basic solution of sodium hydroxide (1mmol) with water (15ml) and then the benzene sulfonyl chloride (1mmol) was added dropwise. The reaction was activated by sonication for 10min at roomtemperature. Subsequently, after the completion of the sulfonylation reaction as monitored by TLC, the p-chlorobenzaldoxime (1.2mmol), oxone (2mmol) and sodium hydroxide (1mmol) were added to the solution mixture at the same temperature to obtain after30min of US irradiation the corresponding cycloadduct (TLC

Preprints (www.preprints.org) | NOT PEER-REVIEWED | Posted: 11 September 2023 doi:10.20944/preprints202309.0671.v1

monitoring). The organic 213 layer was extracted with DCM (3 × 10 mL) and then dried over sodium sulfate, filtred and 214concentrated in vacuum. Recrystallization was employed to purify the crude product in 215 hot ethanol and provide the desired (3-(4-chlorophenyl)-4,5-dihydroisoxazol-5-yl)methyl 216 benzenesulfonate in high purity.

Yield 85%, Mp 121–123°C (Ethanol), TLC (cyclohexane 90%/Ethylacetate 10%) Rf = 0.6; FT-IR (ATR, cm^{-1}): 1660 (C=N), 1190 (O=S=O), 906 (N-O) ; ^{1}H NMR (500 MHz, $DMSOd_6$) δ 7.88 (d, J = 7.2 Hz, 2H, Har), 7.76 (t, J = 7.5 Hz, 1H, Har), 7.64 (t, J = 7.9 Hz, 2H, Har), 7.59 (d, J = 8.6 Hz, 2H, Har), 7.47 (d, J = 8.6 Hz, 2H, Har), 4.95 – 4.89 (m, 1H, C5H-isoxazoline), 4.19 (dd, J = 11.1, 3.1 Hz, 1H, O-CH), 4.14 (dd, J = 11.1, 5.9 Hz, 1H, O-CH), 3.47 (dd, J = 17.3, 11.2 Hz, 1H, C4H-isoxazoline), 3.12 (dd, J = 17.3, 7.1 Hz, 1H, C4H-isoxazoline). ^{13}C NMR (126 MHz, DMSO-d_6) δ 156.3, 135.5, 135.3, 135.0, 130.3(2C), 129.4(2C), 128.9(2C), 128.3, 128.2(2C), 78.5 (CH-isoxazoline), 71.6 (O-CH_2), 36.6 (CH_2-isoxazoline). MS (ESI^+): m/z = 352.3 $[M + H]^+$, 725.7 $[M + Na]^+$.

3.3. X-ray Crystal Structure Data

Table 4 provides data collection, crystal data and refined structural informations. F2 has been improved to combat ALL reflections. The traditional R-factors based on F, are calculated with F set to zero for negative F2, and the weighted R-factor wR and goodness of fit S are based on F2. The selection of reflections for refinement is unrelated to expression at threshold of F2 > 2 sigma(F2), which is utilized solely for computing R-factors(gt) etc. R-factors based on F2 will be statistically even larger than those based on F, which are statistically nearly twice as large. With determined positions (C—H = 0.95-0.99 Å) and riding contributions with isotropic displacement values 1.2-1.5 times that of the linked atoms, H-atoms connected to carbon were positioned in the correct positions.

Table 4. Details of the experiment.

Crystal data	
CCDC Number	2288360
Empirical formula	$C_{16}H_{14}ClNO_4S$
Formula weight	351.79
Temperature/K	150
Crystal system and Space group	Orthorhombic, *Pbca*
a, b, c (Å)	9.5722 (11), 15.0133 (17), 21.978 (2)
α, β, γ (°)	90, 90, 90
Volume ($Å^3$)	3158.5 (6)
Z	8
Radiation type	Mo Kα
μ (mm^{-1})	0.39
Crystal size (mm)	0.30 × 0.25 × 0.16
Data collection	
Diffractometer	diffractometer Bruker D8 QUEST PHOTON 3
Absorption correction	Numerical mu Calculated SADABS [40]
*T*min, *T*max	0.89, 0.94
No. of measured, independent and observed [I > 2σ(I)] reflections	68386, 5453, 4943
*R*int	0.032
(sin θ/λ)max ($Å^{-1}$)	0.748
Refinement	
R[F2 > 2σ(F2)], wR(F2), S	0.032, 0.093, 1.07
No. of reflections	5453
No. of parameters	208

 doi:10.20944/preprints202309.0671.v1

No. of restraints	0
H-atom treatment	H-atom parameters constrained
Δϱmax, Δϱmin (e Å^{-3})	0.41, −0.34

Software applications: SHELXTL [28], SAINT [28], APEX4 [28], SHELXT [29], SHELXL [30], DIAMOND [41].

4. Conclusions

In summary, we proposed an efficient and facile route to synthesize (3-(4-chlorophenyl)-4,5-dihydroisoxazol-5-yl)methyl benzenesulfonate **5** in water using an environmentally friendly protocol involving a one-pot strategy combined with ultrasound cavitation. The desired product (**5**) was obtained in good yield and high purity, and its structure was determined by 1H, 13C NMR, ESI+-MS and IR spectra and confirmed by singlecrystal X-ray diffraction. The Hirshfeld surface has been used to elaborate on the research of intra- and intermolecular interactions, and a comparative theoretical analysis has also been detailed.

Supplementary Materials: The following supporting information can be downloaded at the website of this paper posted on Preprints.org. The following supporting materials, containing 1H, 13C NMR, mass spectra and IR (See SM. Figures S1–S4) of the synthesized compound (**5**) can be downloaded online.

Author Contributions: Conceptualization, approach, writing and original draft research, K.B, L.M., M.D.and K.C.; X-ray crystallography experimentations and structural analyses carried out by X.Z.; Hirshfeld surface investigation and spectroscopic studies completed by K.C. Investigation, writing, review and editing, K.B. All authors have reviewed and agreed with the manuscript's final version.

Funding: This work received no external funding support.

Data Availability Statement**:** Not applicable.

Acknowledgments: This work is supported by UM5R and UM6P. The authors thank UATRSCNRST Morocco.

Conflicts of Interest: The authors declare no conflict of interest.

References

1. Aarjane, M.; Slassi, S.; Ghaleb, A.; Tazi, B.; Amine, A. Synthesis, biological evaluation, molecular docking and in silico ADMET screening studies of novel isoxazoline derivatives from acridone. Arab. J. Chem. 2021, 14, 103057-103069.
2. Kudryavtseva, T. N.; Lamanov, A. Y.; Sysoev, P. I.; Klimova, L. G. Synthesis and antibacterial activity of new acridone derivatives containing an isoxazoline fragment. Russ. J. Gen. Chem. 2020, 90, 45-49.
3. Chalkha, M.; Nour, H.; Chebbac, K.; Nakkabi, A.; Bahsis, L.; Bakhouch, M.; Akhazzane, M.; Bourass, M.; Chtita, S.; Bin Jardan, A. Y.; Augustyniak, M.; Bourhia, M.; Aboul-Soud, M. A. M.; El Yazidi, M. Synthesis, Characterization, DFT Mechanistic Study, Antimicrobial Activity, Molecular Modeling, and ADMET Properties of Novel Pyrazole-isoxazoline Hybrids. ACS omega 2022, 7, 46731-46744.
4. Rasool, J. U.; Sawhney, G.; Shaikh, M.; Nalli, Y.; Madishetti, S.; Ahmed, Z.; Ali, A. Site selective synthesis and anti-inflammatory evaluation of Spiro-isoxazoline stitched adducts of arteannuin. B. Bioorg. Chem. 2021, 117, 105408-105417.
5. Shaik, A.; Bhandare, R. R.; Palleapati, K.; Nissankararao, S.; Kancharlapalli, V.; Shaik, S. Antimicrobial, antioxidant, and anticancer activities of some novel isoxazole ring containing chalcone and dihydropyrazole derivatives. Mol. 2020, 25, 1047-057.
6. Bernal, C. C.; Vesga, L. C.; Mendez-Sánchez, S. C.; Romero Bohórquez, A. R. Synthesis and anticancer activity of new tetrahydroquinoline hybrid derivatives tethered to isoxazoline moiety. Med. Chem. Res. 2020, 29, 675-689.
7. Goyard, D.; Kónya, B.; Chajistamatiou, A. S.; Chrysina, E. D.; Leroy, J.; Balzarin, S.; Maurel, P. Glucose-derived spiro- 276 isoxazolines are anti-hyperglycemic agents against type 2 diabetes through glycogen phosphorylase inhibition. Eur. J. Med. 277 Chem. 2016, 108, 444-454.
8. Huang, M.; Suk, D. H.; Cho, N. C.; Bhattarai, D.; Kang, S. B.; Kim, Y.; Keum, G. Synthesis and biological evaluation of isooxazoline derivatives as potent M1 muscarinic acetylcholine receptor agonists. Bioorg. Med. Chem. Lett. 2015, 25, 1546-1551.

9. Yang, J.; Guan, A.; Wu, Q.; Cui, D.; Liu, C. Design, synthesis and herbicidal evaluation of novel uracil derivatives containing an isoxazoline moiety. Pest Manag. Sci. 2020, 76, 3395-3402.
10. Jiang, B.; Feng, D.; Li, F.; Luo, Y.; He, S.; Dong, Y.; Hu, D. Design, Synthesis, and Insecticidal Activity of Novel Isoxazoline Compounds That Contain Meta-diamides against Fall Armyworm (Spodoptera frugiperda). J. Agric. Food Chem. 2023, 71, 1091-1099.
11. Zhang, C.; Yuan, H.; Hu, Y.; Li, X.; Gao, Y.; Ma, Z.; Lei, P. Structural Diversity Design, Synthesis, and Insecticidal Activity Analysis of Ester-Containing Isoxazoline Derivatives Acting on the GABA Receptor. J. Agric. Food Chem. 2023, 71, 3184-3191.
12. Mahmoudi, A. E.; Fegrouche, R.; Tachallait, H.; Lumaret, J. P.; Arshad, S.; Karrouchi, K.; Bougrin, K. Green Synthesis, Characterization, and Biochemical Impacts of New Bioactive Isoxazoline-sulfonamides as Potential Insecticidal Agents against the Sphodroxia Maroccana Ley. Pest Manag. Sci. 2023.
13. Shan, X.; Lv, M.; Wang, J.; Qin, Y.; Xu, H. Acaricidal and insecticidal efficacy of new esters derivatives of a natural coumarinosthole. Ind. Crops Prod. 2022, 182, 114855-114862.
14. Krishna, P. Chemoselective synthesis of 5-Amino-7-Bromoquinolin-8-Yl Sulfonate derivatives and their antimicrobial evaluation. Phosphorus Sulfur Silicon Relat. Elem. 2018, 193, 685-690.
15. Kanabar, D.; Farrales, P.; Gnanamony, M.; Almasri, J.; Abo-Ali, E. M.; Otmankel, Y.; Shaha, H.; Nguyen, D.; Menyewia, M. E.; Dukhande, V. V.; D'Souzac, A.; Muth, A. Structural modification of the aryl sulfonate ester of cjoc42 for enhanced gankyrin binding and anti-cancer activity. Bioorganic Med. Chem. Lett. 2020, 30, 126889-126893.
16. Xie, D.; Yang, Z.; Hu, X.; Wen, Y. Synthesis, antibacterial and insecticidal activities of novel capsaicin derivatives containing a sulfonic acid esters moiety. Front. Chem. 2022, 10, 929050-929057.
17. Yu, M.; Liu, G.; Zhang, Y.; Feng, T.; Xu, M.; Xu, H. Design, synthesis and evaluation of novel isoxazolines/oxime sulfonates of 2′(2′, 6′)-(di) chloropodophyllotoxins as insecticidal agents. Sci. Rep. 2016, 6, 33062-33073.
18. Zhang, C.; Yuan, H.; Hu, Y.; Li, X.; Gao, Y.; Ma, Z.; Lei, P. Structural Diversity Design, Synthesis, and Insecticidal Activity Analysis of Ester-Containing Isoxazoline Derivatives Acting on the GABA Receptor. J. Agric. Food Chem. 2023, 71, 3184-3191.
19. Liao, J.; Ouyang, L.; Jin, Q.; Zhang, J.; Luo, R. Recent advances in the oxime-participating synthesis of isoxazolines. Org. Biomol. Chem.2020, 18, 4709-4716.
20. Liu, Y.; Meng, J.; Li, C.; Lin, L.; Xu, Y. Progress in the Synthesis of Isoxazoline Derivatives by Cycloylation of AllyOxime. Chinese J. Org. Chem. 2020, 40, 2742.
21. Rane, D.; Sibi, M. Recent advances in nitrile oxide cycloadditions. Synthesis of isoxazolines. Curr. Org. Synth. 2011, 8, 616-627.
22. Lei, X.; Jalla, A.; Abou Shama, M. A.; Stafford, J. M.; Cao, B. Chromatography-free and eco-friendly synthesis of aryl tosylates and mesylates. Synthesis 2015, 2578-2585.
23. Alaoui, S.; Driowya, M.; Demange, L.; Benhida, R.; Bougrin, K. Ultrasound-assisted facile one-pot sequential synthesis of novel sulfonamide-isoxazoles using cerium (IV) ammonium nitrate (CAN) as an efficient oxidant in aqueous medium. Ultrason Sonochem. 2018, 40, 289-297.
24. Talha, A.; Favreau, C.; Bourgoin, M.; Robert, G.; Auberger, P.; Ammari, L. E.; Saadi, M.; Benhida, R.; Martin, A. R.; Bougrin, K. Ultrasound-assisted one-pot three-component synthesis of new isoxazolines bearing sulfonamides and their evaluation against hematological malignancies. Ultrason. Sonochem. 2021, 78, 105748-105759.
25. El Mahmoudi, A.; Chkirate, K.; Tachallait, H.; Van Meervelt, L; Bougrin, K. 2-((3-(4-Methoxyphenyl)-4,5-dihydroisoxazol-5-yl)methyl)benzo[d]isothiazol-3(2H)-one1,1-dioxide. Molbank 2022, M1488. https://doi.org/10.3390/M1488.
26. El Mahmoudi, A.; Chkirate, K. ; Mokhi, L. ; Mague, J.T. ; Bougrin, K. 2-(N-allylsulfamoyl)-N-propylbenzamide. Molbank 2023, M1678.
27. Thari, F. Z.; Tachallait, H.; El Alaoui, N. E.; Talha, A.; Arshad, S.; Álvarez, E.; Karrouchi, K.; Bougrin, K. Ultrasound-assisted one-pot green synthesis of new N-substituted-5-arylidene-thiazolidine-2, 4-dione-isoxazoline derivatives using NaCl/Oxone/Na3PO4 in aqueous media. Ultrason. Sonochem. 2020, 68, 105222-105251.
28. Bruker. APEX4, SAINT & SHELXTL, Bruker AXS LLC, Madison, WI. 2021.
29. Sheldrick, G.M. SHELXT - Integrated space-group and crystal-structure determination. Acta Cryst. A 2015, 71, 3-8.
30. Sheldrick, G.M. Crystal structure refinement with SHELXL. Acta Cryst. C 2015, 71, 3-8.
31. Hirshfeld, F.L. Bonded-atom fragments for describing molecular charge densities. Theor. Chim. Acta 1977, 44, 129–138.
32. Spackman, M.A.; Jayatilaka, D. Hirshfeld surface analysis. Cryst. Eng. Comm. 2009, 11, 19–32.
33. Turner, M.J.; McKinnon, J.J.; Wolff, S.K.; Grimwood, D.J.; Spackman, P.R.; Jayatilaka, D. & Spackman, M.A. CrystalExplorer17. The University of Western Australia 2017.

34. McKinnon, J.J.; Jayatilaka, D. Spackman, M.A. Towards quantitative analysis of intermolecular interactions with Hirshfeld surfaces. Chem. Commun. 2007, 3814–3816.
35. Becke, A.D. Density-functional thermochemistry. III. The role of exact exchange. J. Chem. Phys. 1993, 98, 5648–5652.
36. Lee, C.; Yang, W. Parr, R.G. Development of the Colle-Salvetti correlation-energy formula into a functional of the electron density. Phys. Rev. B 1988, 37, 785–789.
37. Frisch, M.J.; Trucks, G.W. et al. D.J. GAUSSIAN09. Revision A.02. Gaussian Inc, Wallingford, CT, USA 2009.
38. Chkirate, K.; Essassi, E.M. Pyrazole and Benzimidazole Derivatives: Chelating Properties Towards Metals Ions and their Applications. Curr. Org. Chem. 2022, 26(19), 1735 – 1766.
39. Faraj, I.; Oubella, A.; Chkirate, K.; Al Mamari, K.; Hökelek, T.; Mague, J.T.; El Ghayati, L.; Sebbar, N.K.; Essassi, E.M. Crystal 339 structure, Hirshfeld surface analysis and DFT calculations of (E)-3-[1-(2-hydroxyphenylanilino)ethylidene]-6-methylpyran-2,4- 340dione. Acta Cryst. E 2022, 78, 864–870.
40. Krause, L.; Herbst-Irmer, R.; Sheldrick, G.M.; Stalke, D. Comparison of silver and molybdenum microfocus X-ray sources for single-crystal structure determination. J. Appl. Cryst. 2015, 48, 3-10.
41. Brandenburg, K.; Putz, H. DIAMOND. Crystal Impact GbR, Bonn, Germany. 2012.